Model Identification of Distributed Energy Resources using Sparse Regression and Koopman Theory

1st Javad Khazaei
Electrical and Computer Engineering
Lehigh University
Middletown, PA, U.S.
khazaei@lehigh.edu

2nd Faegheh Moazeni
Civil and Environmental Engineering
Lehigh University
Bethlehem, PA , U.S.
moazeni@lehigh.edu

***Abstract*—A complex physics-based modeling procedure and the uncertainty and confidentiality of internal parameters of distributed energy resources (DERs) motivate system identification tools. With the availability of high-fidelity measurements and historical data, model-free identification of DERs can facilitate the control design without tedious modeling of these nonlinear systems. This paper develops a framework for data-driven nonlinear modeling of DERs using sparse identification of nonlinear dynamics (SINDy). In addition, to avoid the complexities of nonlinear control designs, the identified nonlinear dynamics will be lifted to a linear space utilizing Koopman theory. Compared with existing physics-based designs that heavily rely on knowing the detailed system dynamics or data-driven designs that relay on large historical data and are not interpretable, the proposed model-free DER identification framework can accurately capture the dynamics of the DERs with available measurements and lift them to a linear space that provides guaranteed performance for tracking problems. Time-domain simulations were carried out to validate the effectiveness of the proposed approach.**

***Keywords*—** Distributed Energy Resources, Sparse Identification, Koopman Theory, Data-driven System Identification.

I. Introduction

MODELING of distribution systems and microgrids is typically conducted assuming a full knowledge of analytical models of distributed energy resources (DERs), also known as white-box models [1]. In spite of this, detailed information about converter parameters is rarely available with commercial off-the-shelf DERs. Furthermore, DER dynamics are subject to change with aging and faults, which motivates utilizing system identification techniques through leveraging measurement data [2]. The application of system identification tools to DERs stems from the need to create models for control design, stability monitoring, and interconnection studies, such as microgrids.

Several system identification tools have been studied for DERs including black-box and gray-box modeling techniques. To identify a system, black-box modeling assumes no prior knowledge of its topology or analytical equations [3], [4]. Due to inherent nonlinear characteristics of DERs, polytopic and Hammerstein black-box methods have been widely utilized for DERs. Polytopic methods combine multiple weighted neighboring linear models of a converter to estimate a nonlinear behavioral model [5]–[7]. In the Hammerstein method, the combination of non-linear static and linear dynamic models are leveraged to identify non-linear dynamics [8], which is proved to fail against large-signal disturbances [9]. Nevertheless, both Hammerstein and polytopic methods rely heavily on linear methods to estimate nonlinear dynamics, making them dependent upon the DER's operating point and thus unable to capture full nonlinear dynamics. Non-linear black-box modeling methods based on wavelet and dynamic neural networks was proposed in [1], [10], respectively. However, neural networks-based identification methods have several drawbacks, such as their cost, the need for a large number of training data points, and the lack of physical interpretation.

Grey-box identification methods rely on partial knowledge of the system model and dynamics, which then serves as a foundation to estimate the complete model of the system [11]–[13]. This method, however, requires prior knowledge of DER's parametric dynamic equations as well as a lengthy training period and high computational costs.

The availability of high-resolution historical records and advances in machine learning approaches have revolutionized data-driven systems modeling in recent years. A number of approaches have been introduced for capturing the dynamics of complex dynamical systems including: (i) dynamic mode decomposition [14], [15], which heavily relies on a linear dynamics assumption but can handle high-dimensional data, (ii) Koopman operator with control [16], [17] that connects dynamic mode decomposition to nonlinear dynamics through an infinite-dimensional Koopman linear operator, or (iii) sparse identification of system dynamics (SINDy) that uses a sparse regression technique to identify dominant dynamics of candidate functions, and has shown promise in accurately modeling the unknown dynamics of nonlinear systems [18],

This research was in part under support from the National Science Foundation under Grant NSF-EPCN 2221784. The authors are with the college of Engineering at Lehigh University, Bethlehem, PA 18015 USA.

[19]. A major advantage of SINDy is the sparsity technique, which reduces the training time and reduces the reliance on neural networks for control and identification. We have also shown in our preliminary results that sparse identification can capture dynamics of feedback control systems in nonlinear dynamics for accurate distributed control designs [20]. While the existing research shows the significant potential of data-driven approaches such as SINDy and Koopman for identifying nonlinear dynamics of dynamical systems, their application for DER control have not been reported yet.

To address the existing knowledge gaps for identifying DER dynamics in smart grids, this paper investigates the application of sparse identification theory for identification of nonlinear dynamics of DERs using measurements. The learned nonlinear dynamics can then be used to transform the data-driven model into a linear space utilizing Koopman theory. Such linear approximation can significantly reduce the complexities of nonlinear control designs for DERs. Contributions of the paper are listed as:

- Identifying nonlinear dynamics of DERs using data-driven sparse regression technique
- Lifting the nonlinear dynamics of DERs to a linear space using Koopman theory
- Evaluating the effectiveness of a data-driven linear approximation of DER models with physical models through time-domain simulations

The rest of the paper is organized as follows: Section II formulates the DER modeling problem. Sparse identification of DER dynamics is included in Section III. Section IV covers the identification of DER dynamics using Koopman theory. Time-domain simulations are included in Section V and Section VI concludes the paper.

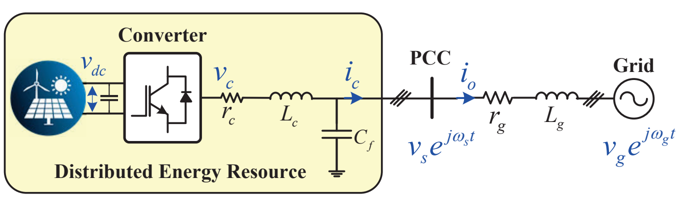

Figure. 1 A DER connected to the grid.

II. Problem Formulation

A DER is shown in Figure. 1 with its power electronics interface (converter) and filtering component (RLC filter), which is connected to the main electricity grid at the point of common coupling (PCC). The power converter is mainly composed of a voltage source DC/AC converter fed by the energy resource (solar, wind, or battery) through a DC link . Each DER unit can be controlled as an AC voltage source through an adjustable voltage magnitude and angle at the PCC, $v_s e^{j\omega_s t}$ [21]. This is achieved through inner current regulators as explained in [22]. Therefore, the variables v_s and ω_s determine the forced response of the DER unit and therefore, are considered as the input variables of the dynamic model. Similarly, the rest of the grid can also be assumed to behave as an AC voltage source modeled as a lumped AC voltage source $v_g e^{j\omega_g t}$ with a series impedance [21]. In the grid-connected mode, v_g and ω_g can be assumed to have fixed values, but in the off-grid mode, these are dynamic variables. It was shown that the lumped model presented in [21] can accurately capture the transient interaction between the DER and the rest of the grid, and therefore, it has been adopted in our study.

A. Lumped Dynamic Model of DERs

The lumped model in Figure. 1 can be represented by the following set of differential equations assuming a synchronous reference frame is aligned with v_s [21]:

$$L_g \frac{d\boldsymbol{i}_o}{dt} = -r_g \boldsymbol{i}_o - j\omega_s L_g \boldsymbol{i}_o - v_g e^{j\delta} + v_s \tag{1}$$

$$\frac{d\delta}{dt} = \omega_g - \omega_s \tag{2}$$

where r_c, L_c, C_f are filter components of the converter, r_g and L_g are the grid impedance components, v_s is the converter voltage at the PCC, v_g is the grid voltage, i_c is the converter current, and i_o is the output current. It is noted that the angle δ is a state variable of the model, which cannot be directly measured and needs to be estimated by a state observer [21]. By decomposing equation (1) into the real and imaginary parts and writing the model in state-space form,

$$\dot{\mathbf{x}} = \mathbf{f}(\mathbf{x}) + \mathbf{g}(\mathbf{x})\mathbf{u}, \qquad \mathbf{y} = \mathbf{h}(\mathbf{x}) \tag{3}$$

where

$$\mathbf{f}(\mathbf{x}) = \begin{bmatrix} -\frac{r_g}{L_g}x_1 - \frac{v_g}{L_g}\cos x_3 \\ -\frac{r_g}{L_g}x_2 - \frac{v_g}{L_g}\sin x_3 \\ \omega_g \end{bmatrix} \tag{4}$$

$$\mathbf{g}(\mathbf{x}) = \begin{bmatrix} \frac{1}{L_g} & x_2 \\ 0 & -x_1 \\ 0 & -1 \end{bmatrix}, \qquad \mathbf{h}(\mathbf{x}) = \begin{bmatrix} x_1 \\ x_2 \end{bmatrix} \tag{5}$$

In equations (3)-(5), $\mathbf{x} = [i_{od}\ i_{oq}\ \delta]^T$ is the state vector, $\mathbf{y} = [i_{od}\ i_{oq}]^T$ is the output vector, and $\mathbf{u} = [v_s\ \omega_s]^T$ is the input vector of the DER unit, which includes the amplitude and voltage angle at the PCC.

B. Data-Driven Model Identification

Assuming detailed information about DERs and their converter parameters are not available, the objective is to identify the lumped dynamic model of DERs in equations (3)-(5) from available measurements of the states. We will utilize sparse identification of nonlinear dynamics (SINDy) to identify equations (3)-(5) from measurements. Next, since the identified model will be nonlinear (referring to equations (3)-(5)), we will utilize Koopman spectral theory to transform the identified nonlinear dynamics to an infinite-dimension linear system. The linear model can then be utilized for designing optimal control laws that guarantee the performance

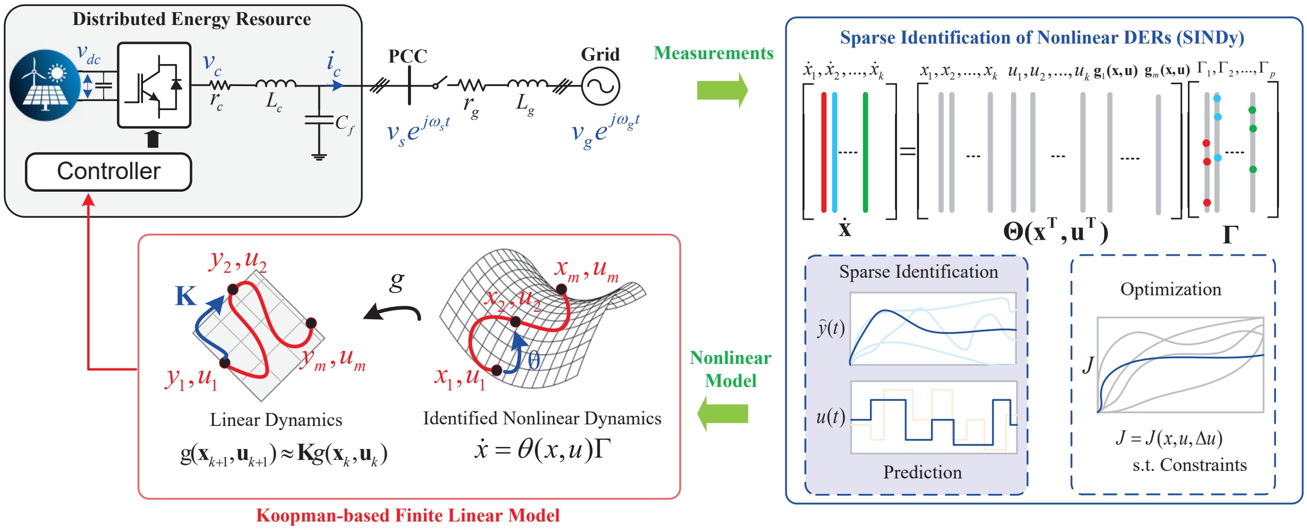

Figure. 2 Identified DER dynamics using SINDy.

of the DERs in various grid conditions. An overview of the proposed approach for data-driven Koopman model identification of DERs is depicted in Figure. 2. As it can be seen, by utilizing a full state feedback from the DERs, a sequentially thresholded least-square optimization problem is solved to obtain the nonlinear dynamics of DERs from the data using sparse regression technique. The identified model will then be transformed to an infinite-dimension linear system using Koopman operator (**K**), which can then be used for optimal control design purposes.

III. Model-Free Identification of DERs

To identify nonlinear/linear systems' governing equations, we construct families of candidate functions that describe how state variables change over time. Since most dynamical systems have few nonlinear terms in the dynamics, sparsity promoting techniques can identify the candidate functions with the greatest impact on forming the system dynamics. Originally proposed in [18], this method is known as sparse identification of nonlinear dynamics (SINDy). In SINDy, the system dynamics are derived through symbolic regression and sparse representations. A sparse identification relies on the fact that many dynamical systems with the form $\dot{x} = f(x,u)$ have a relatively few terms on the right hand side. We assume that the actual dynamics of a DER is represented by $\dot{\mathbf{x}} = \mathbf{f}(\mathbf{x}) + \mathbf{g}(\mathbf{x})\mathbf{u}$, where $\mathbf{x}(t) \in \mathbb{R}^n$ is the state vector, $\mathbf{u}(t) \in \mathbb{R}^q$ is the input or control vector, and $\mathbf{f}(\mathbf{x}(t), \mathbf{u}(t)) : \mathbb{R}^n \times \mathbb{R}^q \rightarrow \mathbb{R}^n$.

A. Data Collection

By collecting m samples of measurements from the states and inputs, each DER can then be identified by a library of candidate functions, $\Theta \in \mathbb{R}^{m\times p}$. To identify the governing equations of the system in (1), a time-history of the state vector $\mathbf{x}(t)$, input $\mathbf{u}(t)$, and $\dot{\mathbf{x}}(t)$ is required. In most practical systems, only $\mathbf{x}(t)$ and $\mathbf{u}(t)$ are available and $\dot{\mathbf{x}}(t)$ needs to be estimated from $\mathbf{x}(t)$. If the measurement data is sampled at m intervals $t_1,\ t_2,\ \ldots,\ t_m$ and measurements are arranged into a matrix $\mathbf{X}$,

$$\mathbf{X} = \begin{bmatrix} \mathbf{x}^T(t_1) \\ \mathbf{x}^T(t_2) \\ \vdots \\ \mathbf{x}^T(t_m) \end{bmatrix} = \begin{bmatrix} x_1(t_1) & x_2(t_1) & \ldots & x_n(t_1) \\ x_1(t_2) & x_2(t_2) & \ldots & x_n(t_2) \\ \vdots & \vdots & \ddots & \vdots \\ x_1(t_m) & x_2(t_m) & \ldots & x_n(t_m) \end{bmatrix} \tag{6}$$

and inputs for t_m samples are written into a matrix $\mathbf{U}$,

$$\mathbf{U} = \begin{bmatrix} \mathbf{u}^T(t_1) \\ \mathbf{u}^T(t_2) \\ \vdots \\ \mathbf{u}^T(t_m) \end{bmatrix} = \begin{bmatrix} u_1(t_1) & u_2(t_1) & \ldots & u_n(t_1) \\ u_1(t_2) & u_2(t_2) & \ldots & u_n(t_2) \\ \vdots & \vdots & \ddots & \vdots \\ u_1(t_m) & u_2(t_m) & \ldots & u_n(t_m) \end{bmatrix} \tag{7}$$

the measurements for derivatives can be approximated numerically from $\mathbf{X}$.

B. Estimating the Derivatives, $\dot{\mathbf{X}}$

Ordinary and partial differential equations are numerically solved using difference approximation. Considering a smooth function in the neighborhood of point x, the derivatives can be approximated using Taylor series expansion at specified mesh points. As the central difference approximation is more accurate for smooth functions, it is used in this paper. As a result, $\dot{\mathbf{X}}$ can be approximated by [23]:

$$\dot{\mathbf{X}} \approx \frac{\mathbf{X}(i+1) - \mathbf{X}(i-1)}{2h} \tag{8}$$

where $\mathbf{X}(i+1)$ is the measured data at sample $i+1$ and h is the sampling time of the data collection platform.

C. Sparse Identification of System Dynamics

If the measured data $\mathbf{X} \in \mathbb{R}^{m\times n}$ is used to obtain the measured derivatives of the states, the vector of measured derivatives is a linear combination of columns from the candidate function (e.g., polynomials, or sinusoids) library.

$$\Theta(\mathbf{X},\mathbf{U}) = \begin{bmatrix} | & | & | & | & | & & | & | & | & \\ 1 & \mathbf{X} & \mathbf{U} & \mathbf{P_2}(\mathbf{X},\mathbf{U}) & \mathbf{P_3}(\mathbf{X},\mathbf{U}) & \dots & \sin(\mathbf{X},\mathbf{U}) & \cos(\mathbf{X},\mathbf{U}) & \sin(\mathbf{2}(\mathbf{X},\mathbf{U})) & \dots \\ | & | & | & | & | & & | & | & | & \end{bmatrix} \tag{10}$$

The linear combination of columns is expressed by entries of the matrix $\Xi \in \mathbb{R}^{p\times n}$ such that [18]:

$$\dot{\mathbf{X}} = \Theta(\mathbf{X},\mathbf{U})\boldsymbol{\Xi}. \tag{9}$$

Having calculated $\dot{\mathbf{X}}$, the library of candidate functions will be constructed as linear and nonlinear functions of the columns of $\mathbf{X}$ and $\mathbf{U}$. A typical choice of candidate functions include polynomials and trigonometric functions for nonlinear systems as represented in equation (10). In equation (10), $\mathbf{P_i}(\mathbf{X},\mathbf{U})$ denotes a nonlinear combination of i-order polynomials of $\mathbf{X}$ and $\mathbf{U}$. For example, $\mathbf{P_2}(\mathbf{X},\mathbf{U})$ includes polynomials up to second order. In the final step of the identification process, a sparse regression algorithm is employed to solve for the sparse vectors of coefficients in $\boldsymbol{\Xi}$ that decide what terms are active in the $\dot{\mathbf{X}}$ dynamics:

$$\boldsymbol{\xi}_h = \arg\min_{\hat{\boldsymbol{\xi}}_h} ||\dot{\mathbf{X}}_h - \boldsymbol{\Theta}(\mathbf{X},\mathbf{U})\hat{\boldsymbol{\xi}}_h||_2 + \lambda||\hat{\boldsymbol{\xi}}_h||_0 \tag{11}$$

where $\boldsymbol{\xi}_h$ is the h-th column of $\boldsymbol{\xi}$ represented by $\boldsymbol{\xi}_h = \begin{bmatrix}\xi_1 \ \xi_2 \ \dots \ \xi_p\end{bmatrix}^T$ and $\dot{\mathbf{X}}_h$ represents the h-th column of $\dot{\mathbf{X}}$. The objective function in (11) comprises two norm functions. The L2 norm denoted by $||.||_2$, solves for the least-squares problem. The L0 norm, $||.||_0$, decides the number of nonzero elements in $\boldsymbol{\xi}_h$, promoting sparsity in the coefficients matrix and λ is the sparsity-promoting hyperparameter.

The minimization problem of (11) is solved by the sequentially thresholded least squares (STLS) proposed in [24] defined by [25]:

$$S^k = \left\{ j \in [p] : \left|\xi_j^k\right| \geq \lambda \right\}, \quad k \geq 0 \tag{12}$$

$$\hat{\boldsymbol{\xi}}_h^0 = \boldsymbol{\Theta}(\mathbf{X},\mathbf{U})^{\dagger}\dot{\mathbf{X}}_h \tag{13}$$

$$\boldsymbol{\xi}^{k+1} = \underset{\hat{\boldsymbol{\xi}}_h \in \mathbb{R}^p : \mathrm{supp}(\boldsymbol{\xi}_h) \subseteq S^k}{\mathrm{argmin}} ||\dot{\mathbf{X}}_h - \boldsymbol{\Theta}(\mathbf{X},\mathbf{U})\hat{\boldsymbol{\xi}}_h||_2, \tag{14}$$

where k is the iteration number, $\boldsymbol{\Theta}(\mathbf{X},\mathbf{U})^{\dagger}$ is the pseudo-inverse of $\boldsymbol{\Theta}(\mathbf{X},\mathbf{U})$, defined as $\boldsymbol{\Theta}(\mathbf{X},\mathbf{U})^{\dagger} := [\boldsymbol{\Theta}(\mathbf{X},\mathbf{U})^T\boldsymbol{\Theta}(\mathbf{X},\mathbf{U})]^{-1}\boldsymbol{\Theta}(\mathbf{X},\mathbf{U})^T$, and the support set of $\boldsymbol{\xi}_h$ is defined by $\mathrm{supp}(\boldsymbol{\xi}_h) := \{j \in [p] : \xi_j \neq 0\}$. The coefficients of Γ can be found using the sparse regression formulation presented in **Algorithm 1**. If the intent is to identify the signal $\mathbf{U}$ for feedback control, i.e., $\mathbf{U} = G(s)\mathbf{X}$, where $G(s)$ is the transfer function of the controller, the matrix of inputs can be identified using $\mathbf{U} = \Theta(\mathbf{X})\boldsymbol{\Gamma}_\mathbf{u}$, where $\Theta(\mathbf{X})$ is the matrix of candidate functions with the terms corresponding to $\mathbf{U}$ have been removed from $\Theta(\mathbf{X},\mathbf{U})$ and $\boldsymbol{\Gamma}_\mathbf{u}$ can be found using the sparse regression algorithm similar to $\boldsymbol{\Xi}$.

Algorithm 1 Sparse Regression Algorithm

```
Input: Measurements X, U
Input: Estimated derivatives Ẋ
procedure STLS
Γ = Θ\Ẋ (least-square solution)
    for k = 1 : 10 do (number of iterations)
        Set λ (sparcification knob)
        |Ξ| < λ ⟶ ind_small
        Ξ(ind_small) ⟶ 0
        for k = 1 : n do (n dimension of state X)
            ind_big ≠ ind_small(:, k)
            Ξ(ind_big, k) = Θ(:, ind_big)\Ẋ(:, k)
        end for
    end for
Output: sparse matrix Ξ
```

IV. Koopman-based Identification of DER Dynamics

The Koopman operator is a linear operator that provides an analytic and numerical tool to lift nonlinear dynamical systems to an infinite-dimension linear system. Considering a nonlinear dynamical system with external input represented by $\dot{\mathbf{x}} = \mathbf{f}(\mathbf{x},\mathbf{u})$, where $\mathbf{x} \in \mathcal{M}$ and $\mathbf{u} \in \mathcal{N}$ with $\mathcal{M}$ and $\mathcal{N}$ being smooth manifolds [26]. In most practical engineering problems, including power systems, the state and input manifolds are considered as $\mathbf{x} \in \mathbb{R}^n$ and $\mathbf{u} \in \mathbb{R}^q$. A set of scalar-valued observable functions $\mathrm{g}(\mathbf{x},\mathbf{u})$ that depend on the state and input will be defined as $\mathrm{g} : \mathcal{M} \otimes \mathcal{N} \to \mathbb{R}$. Each observable function will be an element of an infinite-dimensional Hilbert space $\mathcal{H}$. The Koopman operator $\mathbf{K} : \mathcal{H} \to \mathcal{H}$ acts on the Hilbert space of observable functions as [26]:

$$\mathbf{K}\mathrm{g}(\mathbf{x},\mathbf{u}) \triangleq \mathbf{K}\mathrm{g}(\mathrm{f}(\mathbf{x},\mathbf{u}),\mathbf{u}) \tag{15}$$

The linear characteristics of Koopman operator allows performing eigendecomposition of $\mathbf{K}$ in a standard form:

$$\mathbf{K}\phi_j(\mathbf{x},\mathbf{u}) = \lambda_i\phi_j(\mathbf{x},\mathbf{u}) \tag{16}$$

which means the Koopman operator is spanned by eigenfunctiopns that are defined by the states and inputs. By rewriting the observable functions $\mathrm{g_i}$ in terms of the right eigenfunctions ϕ_j,

$$\mathrm{g}(\mathbf{x},\mathbf{u}) = \begin{bmatrix} \mathrm{g}_1(\mathbf{x},\mathbf{u}) \\ \mathrm{g}_2(\mathbf{x},\mathbf{u}) \\ \vdots \\ \mathrm{g}_{\mathrm{n_z}}(\mathbf{x},\mathbf{u}) \end{bmatrix} = \sum_{j=1}^{\infty} \phi_j(\mathbf{x},\mathbf{u})\mathbf{v}_j \tag{17}$$

where n_z is the number of measurements and $\mathbf{v}_j$ are the Koopman modes. Considering the dynamics of DERs in equations (3)-(5) and measurement functions defined as $\mathrm{g}(\mathbf{x},\mathbf{u}) = \mathbf{y} = [x_1 \;\; x_2 \;\; x_3 \;\; \cos x_3 \;\; \sin x_3]^T$, the exact Koopman-based model of DERs can be manually calculated without the need for estimating the Koopman-modes. The final model is expressed as:

$$\frac{d}{dt}y_1 = -\frac{r_g}{L_g}y_1 - \frac{v_g}{L_g}y_4 + \frac{1}{L_g}u_1 + y_2u_2 \tag{18}$$

$$\frac{d}{dt}y_2 = -\frac{r_g}{L_g}y_2 - \frac{v_g}{L_g}y_5 - y_1u_2 \tag{19}$$

$$\frac{d}{dt}y_3 = \omega_g - u_2 \tag{20}$$

$$\frac{d}{dt}y_4 = -\omega_g y_5 + y_5u_2 \tag{21}$$

$$\frac{d}{dt}y_5 = \omega_g y_4 - y_4u_2 \tag{22}$$

Knowing that the parameters of the above model are not known, sparse identification will be first utilized to obtain the model in equations (3)-(5) before obtaining the above Koopman model.

V. Case Studies

To validate the effectiveness of the proposed data-enabled model-free Koopman-based DER models, several case studies are carried out. First, sparse identification of DER dynamics is performed by perturbing the inputs of the DER model and capturing measurements. The identified data-driven DER model is then utilized to obtain the Koopman-based DER model. Comparisons with physical models have also been carried out to validate the effectiveness of the proposed identification framework.

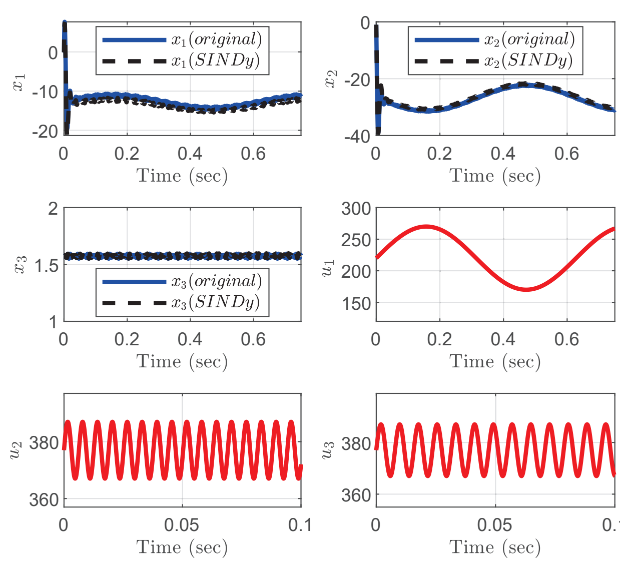

Figure. 3 Identified DER dynamics using SINDY.

A. SINDY-based Identification of DERs

First, data of a DER was collected for 0.8 seconds with 50μsec sampling time (16000 samples) via MATLAB simulations using the parameters provided in [21]. For $\Theta(\mathbf{X},\mathbf{U})$, the candidate terms include polynomials up to degree 2 and sinusoidal functions, i.e., $u_i, x_i, x_ix_j, x_i^2, x_i\cos x_j, x_i \sin x_j, u_i \cos x_j, u_i \sin x_j$. The sparse identification was then carried out to identify the sparse matrix of coefficients, Ξ. The identified Ξ for the studied DER model were used to develop a data-driven DER model in MATLAB. A comparison between the physical model and the identified model is shown in Figure. 3, where $\mathbf{x} = [i_{od} \; i_{oq} \; \delta]^T$ is the state vector and $\mathbf{u} = [v_s \; \omega_s \; \omega_g]^T$ is the input vector of the DER unit. As it can be seen, the identified data-driven model accurately represents the dynamics of the physical model.

B. SINDY-Koopman Identification

In the second case study, the obtained Koopman model of the DER units was compared with the physical model in several scenarios. A step change from 220V to 100V was applied to the grid voltage v_g at 0.25 seconds in all scenarios, that resembles an undervoltage fault. Three scenarios have been considered: i) SINDy: the original model (physical DER model in equations (3)-(5)) was first compared with the identified data-driven model using SINDy, ii) Koopman: the Koopman model was obtained from the original model (physical model in equations (3)-(5)), and iii) SINDy-Koopman: the Koopman model was obtained from the data-driven model using SINDy. Results are shown in Figure. 4. The results show the effectiveness of the proposed data-driven model identification approach (SINDy-Koopman) for accurately identifying the nonlinear dynamics of DERs in smart grid and lifting their nonlinear dynamics to a finite linear space utilizing Koopman theory. Such linear representation can significantly simplify the control design.

VI. Conclusion

In this paper, a model-free Koopman-based identification of DER dynamics was studied. Using sparse identification of nonlinear dynamics with control along with available measurements, dynamics of the DER were predicted with a library of candidate functions. The learned dynamics were then used to lift the nonlinear dynamics to a finite linear space using Koopman theory. The proposed research demonstrates the effectiveness of the sparse identification and Koopman theory for data-driven model identification of nonlinear systems. Such formulation can significantly reduce the existing complexities of control design in modern power systems. Future research will focus on designing optimal control frameworks for DER dispatch in smart grids using Koopman theory.

References

[1] G. Rojas-Dueñas, J.-R. Riba, and M. Moreno-Eguilaz, "Black-box modeling of dc–dc converters based on wavelet convolutional neural networks," *"IEEE Trans. Instrum. Meas."*, vol. 70, pp. 1–9, 2021.

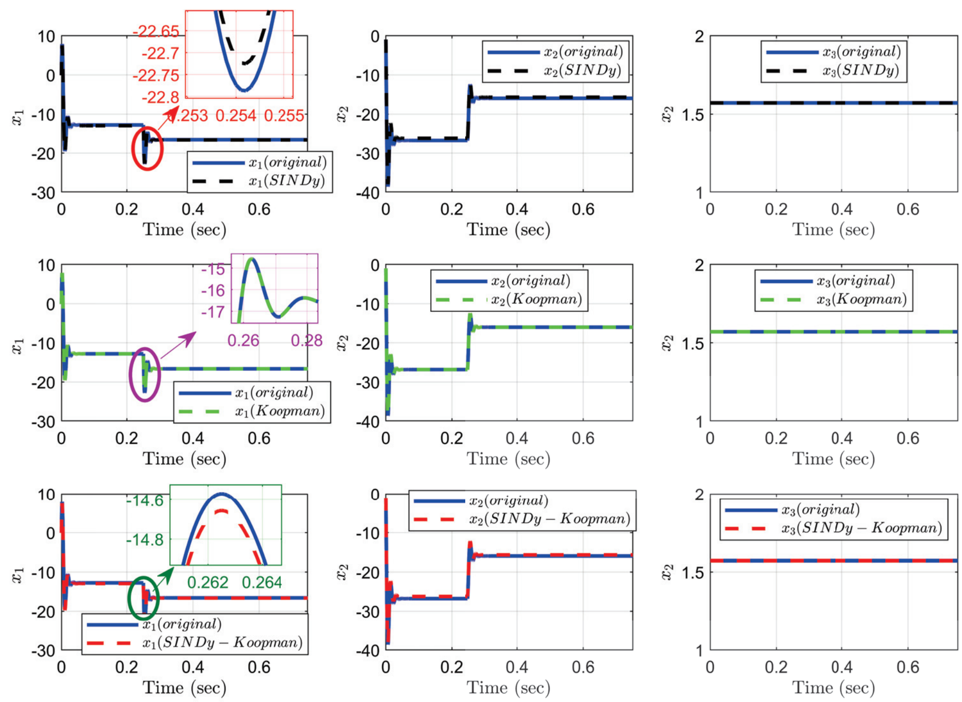

Figure. 4 Identified DER dynamics using SINDy and Koopman.

[2] M. Al-Greer, M. Armstrong, M. Ahmeid, and D. Giaouris, "Advances on system identification techniques for dc–dc switch mode power converter applications," *IEEE Trans. Power Electron.*, vol. 34, no. 7, pp. 6973–6990, 2019.

[3] L. Arnedo, D. Boroyevich, R. Burgos, and F. Wang, "Un-terminated frequency response measurements and model order reduction for black-box terminal characterization models," in *2008 Twenty-Third Annual IEEE Applied Power Electronics Conference and Exposition*, 2008, pp. 1054–1060.

[4] I. Cvetkovic, D. Boroyevich, P. Mattavelli, F. C. Lee, and D. Dong, "Unterminated small-signal behavioral model of dc–dc converters," *IEEE Trans. Power Electron.*, vol. 28, no. 4, pp. 1870–1879, 2013.

[5] L. Arnedo, D. Boroyevich, R. Burgos, and F. Wang, "Polytopic black-box modeling of dc-dc converters," in *2008 IEEE Power Electronics Specialists Conference*, 2008, pp. 1015–1021.

[6] A. Francés, R. Asensi, and J. Uceda, "Blackbox polytopic model with dynamic weighting functions for dc-dc converters," *IEEE Access*, vol. 7, pp. 160 263–160 273, 2019.

[7] V. Valdivia, A. Barrado, A. Lázaro, M. Sanz, D. López del Moral, and C. Raga, "Black-box behavioral modeling and identification of dc–dc converters with input current control for fuel cell power conditioning," *IEEE Trans. Ind. Electron.*, vol. 61, no. 4, pp. 1891–1903, 2014.

[8] F. Alonge, F. D'Ippolito, F. M. Raimondi, and S. Tumminaro, "Nonlinear modeling of dc/dc converters using the hammerstein's approach," *IEEE Trans. Power Electron.*, vol. 22, no. 4, pp. 1210–1221, 2007.

[9] I. Cvetkovic, D. Boroyevich, P. Mattavelli, F. C. Lee, and D. Dong, "Non-linear, hybrid terminal behavioral modeling of a dc-based nanogrid system," in *2011 Twenty-Sixth Annual IEEE Applied Power Electronics Conference and Exposition (APEC)*, 2011, pp. 1251–1258.

[10] A. Wunderlich and E. Santi, "Digital twin models of power electronic converters using dynamic neural networks," in *2021 IEEE Applied Power Electronics Conference and Exposition (APEC)*, 2021, pp. 2369–2376.

[11] A. Francés, R. Asensi, García, R. Prieto, and J. Uceda, "Modeling electronic power converters in smart dc microgrids—an overview," *IEEE Trans. Smart Grid*, vol. 9, no. 6, pp. 6274–6287, 2018.

[12] F. Hafiz, A. Swain, E. M. A. M. Mendes, and L. A. Aguirre, "Multiobjective evolutionary approach to grey-box identification of buck converter," *IEEE Trans. Circuits Syst. I*, vol. 67, no. 6, pp. 2016–2028, 2020.

[13] A. Wunderlich, K. Booth, and E. Santi, "Hybrid analytical and data-driven modeling techniques for digital twin applications," in *2021 IEEE Electric Ship Technologies Symposium (ESTS)*, 2021, pp. 1–7.

[14] M. Liu, L. Tan, and S. Cao, "Method of dynamic mode decomposition and reconstruction with application to a three-stage multiphase pump," *Energy*, vol. 208, p. 118343, 2020.

[15] H. Lu and D. M. Tartakovsky, "Prediction accuracy of dynamic mode decomposition," *SIAM Journal on Scientific Computing*, vol. 42, no. 3, pp. A1639–A1662, 2020.

[16] M. Al-Gabalawy, "Deep learning for koopman operator optimal control," *ISA transactions*, 2021.

[17] A. Mauroy, I. Mezić, and Y. Susuki, *The Koopman Operator in Systems and Control: Concepts, Methodologies, and Applications*. Springer Nature, 2020, vol. 484.

[18] S. L. Brunton, J. L. Proctor, and J. N. Kutz, "Discovering governing equations from data by sparse identification of nonlinear dynamical systems," *Proceedings of the national academy of sciences*, vol. 113, no. 15, pp. 3932–3937, 2016.

[19] ——, "Sparse identification of nonlinear dynamics with control (sindyc)," *IFAC-PapersOnLine*, vol. 49, no. 18, pp. 710–715, 2016.

[20] J. Khazaei and R. S. Blum, "Model-free distributed control of dynamical systems," *International Journal of Information and Communication Engineering*, vol. 16, no. 10, pp. 475–480, 2022.

[21] R. Pérez-Ibacache, C. A. Silva, and A. Yazdani, "Linear state-feedback primary control for enhanced dynamic response of ac microgrids," *IEEE Transactions on Smart Grid*, vol. 10, no. 3, pp. 3149–3161, 2018.

[22] A. Yazdani and R. Iravani, *Voltage-sourced converters in power systems: modeling, control, and applications*. John Wiley & Sons, 2010.

[23] S. Larsson and V. Thomée, *Partial differential equations with numerical methods*. Springer, 2003, vol. 45.

[24] S. L. Brunton, J. L. Proctor, and J. N. Kutz, "Discovering governing equations from data by sparse identification of nonlinear dynamical systems," *Proceedings of the National Academy of Sciences*, vol. 113, no. 15, pp. 3932–3937, 2016.

[25] L. Zhang and H. Schaeffer, "On the convergence of the sindy algorithm," *Multiscale Modeling & Simulation*, vol. 17, no. 3, pp. 948–972, 2019.

[26] E. Kaiser, J. N. Kutz, and S. L. Brunton, "Data-driven discovery of koopman eigenfunctions for control," *Machine Learning: Science and Technology*, vol. 2, no. 3, p. 035023, 2021.